L-2015-053

Enclosure 1

WCAP-17973-NP, Revision 1, "Turkey Point Units 3 and 4 Pressurizer Heater Sleeve Flaw Evaluation to Support Half-Nozzle Repairs" (Non-Proprietary)

WCAP-17973-NP
Revision 1

February 2015

Turkey Point Units 3 and 4 Pressurizer Heater Sleeve Flaw Evaluation to Support Half-Nozzle Repairs

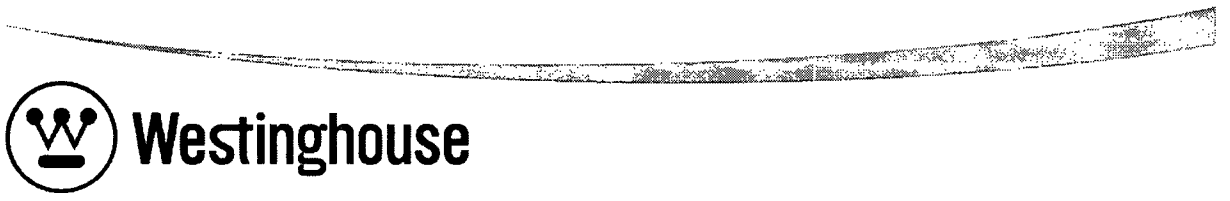

WCAP-17973-NP
Revision 1

Turkey Point Units 3 and 4 Pressurizer Heater Sleeve Flaw Evaluation to Support Half-Nozzle Repairs

Jeffery T. Menard*
Major Reactor Component Design and Analysis - I

Nathan L. Glunt*
Piping Analysis and Fracture Mechanics

February 2015

Reviewer: Gordon Z. Hall*
Major Reactor Component Design and Analysis – I

Reviewer: Anees Udyawar*
Piping Analysis and Fracture Mechanics

Approved: James P. Burke for Carl J. Gimbrone*, Manager
Major Reactor Component Design and Analysis – I

Approved: John L. McFadden*, Manager
Piping Analysis and Fracture Mechanics

Details of contributor roles are attached in EDMS.

*Electronically approved records are authenticated in the electronic document management system.

Westinghouse Electric Company LLC
1000 Westinghouse Drive
Cranberry Township, PA 16066, USA

TABLE OF CONTENTS

LIST OF TABLES

LIST OF FIGURES

1 BACKGROUND AND INTRODUCTION

During the Spring 2014 refueling outage at Florida Power & Light Company Turkey Point Unit 3, visual examinations of the pressurizer heater sleeve penetrations revealed evidence of leakage in the annulus between the outer surface of the heater sleeve and the lower head bore at heater penetration #11. No other leakages were observed from any of the other heater penetrations. Subsequent eddy current inspection conducted from the sleeve bore, after the heater was removed, did not reveal any flaws in the sleeve itself. Therefore, the most likely location of the flaw was determined to be in the stainless steel weld between the heater sleeve and the stainless steel cladding buildup (see Figure 1-1).

The stainless steel heater sleeve is welded with a partial penetration weld to the stainless steel cladding buildup on the inside of the pressurizer lower head. The partial penetration weld joint does not extend into the lower head carbon steel base material. The cladding has two layers, each 0.1875 inch thick, and one of these layers remains beneath the partial penetration weld. Removing, grinding, or machining the stainless weld or the internal surface components of the pressurizer results in high radiation exposure and safety hazards to personnel. Furthermore, repairing the region from the inside diameter could result in foreign material remaining in the pressurizer potentially affecting fuel performance

The "half-nozzle" method was used during the Spring 2014 outage to repair the heater sleeve penetration #11 at Turkey Point Unit 3 as an alternative to ASME Section XI [1] requirement IWB-3142.3 to correct the leakage observed in the heater sleeve region. For the half-nozzle repair, the heater is removed and the heater sleeve is severed below the pressurizer lower head. The remaining lower portion of the heater sleeve is removed by boring to approximately mid-wall of the lower head. The removed portion of the stainless steel sleeve is then replaced with a section (half-nozzle) of low carbon stainless steel which will then be welded to the outside surface of the pressurizer lower head using low carbon stainless steel weld filler. A new heater was then welded to the bottom of the replacement lower sleeve using low carbon stainless steel weld filler. The upper portion of the sleeve, including the partial penetration weld, remained in place. Similar heater sleeve welds on pressurizers with Alloy 600 material have been repaired by the industry using a half-nozzle technique. The half-nozzle method has been used at St. Lucie Unit 2 and many other Combustion Engineering designed NSSS plants.

A relief request [2] by Turkey Point Unit 3 was submitted to and approved by the U.S. Nuclear Regulatory Commission (NRC) for continued operation of the plant for an 18-month fuel cycle with the half-nozzle repair at Penetration #11. The relief request stated: "During the next fuel cycle, additional analyses will be performed to justify the revised configuration with the postulated flaw(s) remaining in place for the current inspection interval for Turkey Point Unit 3 which expires on February 21, 2024." The evaluation performed in this report will demonstrate the acceptability of the half-nozzle repair for any flawed heater sleeve penetration welds at Turkey Point Units 3 and 4 based on ASME Section XI crack growth analysis and a flaw stability analysis. The flaw evaluation will demonstrate that any flaws in the partial penetration weld will not grow to an unacceptable flaw size into the lower head base metal, for up to 40 years of operation, based on both fatigue and corrosion crack growth mechanisms. The flaw evaluation discussed herein is applicable to all heater sleeve penetration locations in the pressurizer lower

head. Furthermore, since the geometry, material, and operating parameters for Turkey Point Units 3 and 4 are the same, the evaluation applies to both units.

To support the fracture mechanics evaluation, a plant-specific stress analysis of the pressurizer heater sleeve region was conducted. Finite element modeling was performed to solve for the temperature and stress response of the pressurizer lower head at the heater sleeve region due to the operating conditions and design transients (Section 2) for Turkey Point Units 3 and 4. The stress results from the finite element modeling discussed in Section 3 were then inputted into a fracture mechanics evaluation.

The fracture evaluation described in Section 4 provides a crack growth chart for the pressurizer heater sleeve location with an assumed flawed partial penetration weld. The postulated flaw is assumed to cover the entire partial penetration weld including the depth of the two layers of stainless steel cladding; therefore, the crack front is at the interface between the cladding and the pressurizer lower head base metal. Both fatigue and corrosion crack growth are considered in the evaluation to demonstrate that the flaw will not reach the ASME Section XI maximum end-of-evaluation flaw size in 20 and 40-year evaluation periods. Both Turkey Point Units 3 and 4 have less than 40 years of operation remaining; therefore, the fracture mechanics evaluation bounds the entire operating life for both units.

Portions of this report contain proprietary information. Proprietary information is identified and bracketed. For each of the bracketed sections, the reasons for the proprietary classification are provided using superscripted letters "a", "c", and "e". These letter designations are:

a. The information reveals the distinguishing aspects of a process or component, structure, tool, method, etc. The prevention of its use by Westinghouse's competitors, without license from Westinghouse, gives Westinghouse a competitive economic advantage.

c. The information, if used by a competitor, would reduce the competitor's expenditure of resources or improve the competitor's advantage in the design, manufacture, shipment, installation, assurance of quality, or licensing of a similar product.

e. The information reveals aspects of past, present, or future Westinghouse- or customer-funded development plans and programs of potential commercial value to Westinghouse.

Revision 0 is superseded by Revision 1, there are no technical changes between Revisions 0 and 1.

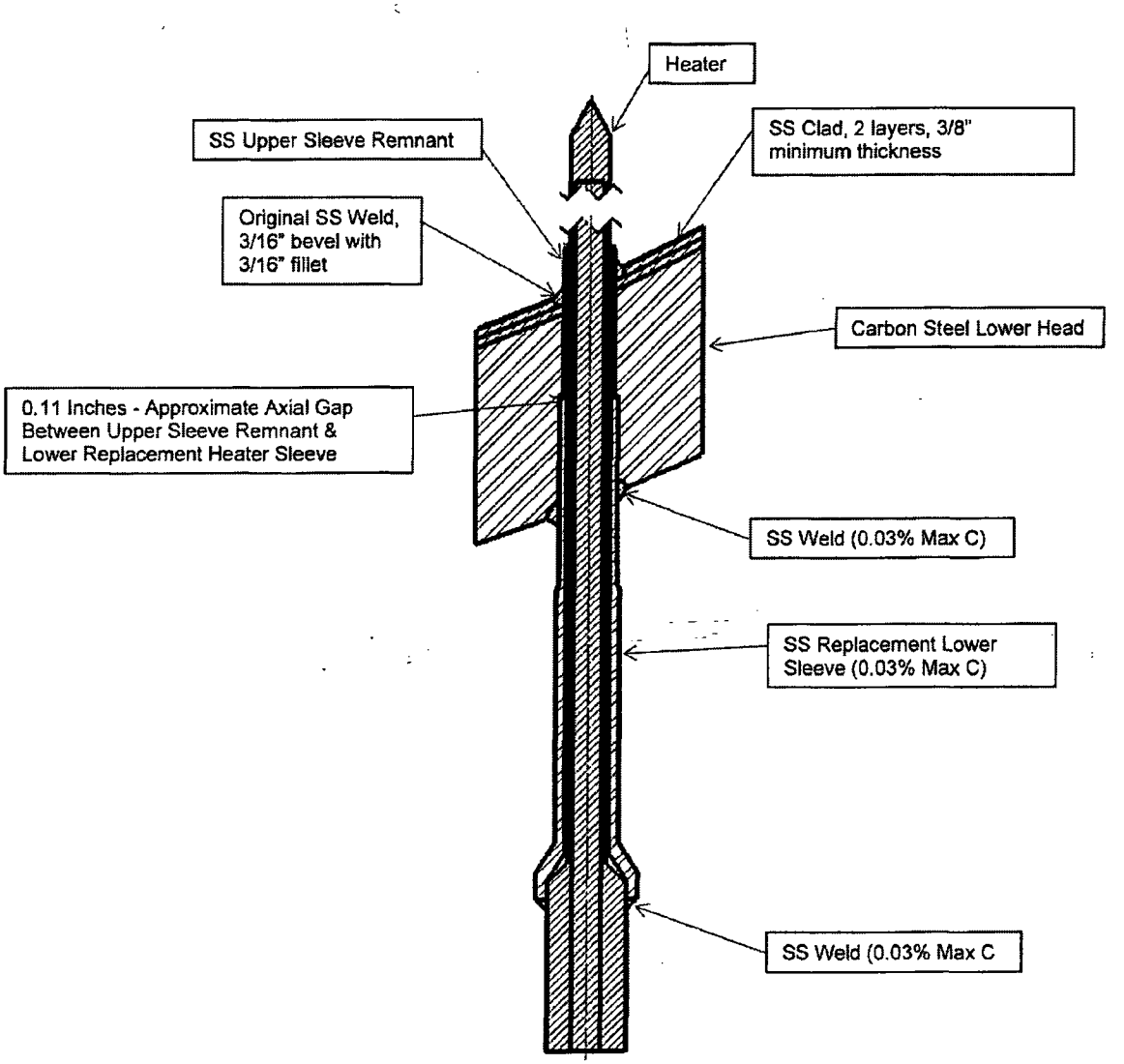

Figure 1-1 Penetration #11 Final Configuration

2 THERMAL AND PRESSURE TRANSIENT CONSIDERATIONS

The fracture mechanics evaluation based on ASME Section XI requires the calculation of flaw growth for the remaining life of the plants, along with the determination of the maximum allowable flaw size. Both fatigue and corrosion crack growth mechanisms are considered for flaw growth through the head material. The corrosion growth rate is discussed in Section 4.3 and is incorporated along with the fatigue crack growth as part of the fracture mechanics evaluation. A complete discussion of fatigue crack growth is also provided in Section 4.3. The fatigue crack growth and maximum allowable flaw size calculations require thermal and pressure transient stresses and the associated cycles based on the plant-specific design transients as input. The consideration of thermal and pressure transients used to calculate the through-wall time history stresses for the Turkey Point Units 3 and 4 pressurizer lower head region is discussed herein.

The current Turkey Point Units 3 and 4 pressurizer design transients are based on the extended power uprate (EPU) [3 through 6]. The transients and cycles are listed in Table 2-1. Pressurizer fluid temperatures for certain transients, such as inadvertent auxiliary spray, turbine roll tests, and steam line break, are based on saturation conditions per [6]. Additionally, per [7], the initial hydrostatic pressure test is not necessary for the Section XI flaw evaluation.

Per [7], Turkey Point Units 3 and 4 operate according to the modified steam bubble method described in [8]. Therefore, the modified operating procedure (MOP) insurge/outsurge (I/O) transients described in [8] are applicable herein. The MOP I/O transient shape described in [8] is shown in Figure 2-1. The MOP I/O transient cycles per [8] are shown in Table 2-2.

Table 2-1 List of Pressurizer Design Transients for Turkey Point Units 3 and 4 EPU [3]

Transient Description		Design Cycles Applicable for 60 Years
Normal Condition		
1	Plant Heatup	200
2	Plant Cooldown	200
3	Plant Loading at 5% of Full Power per Minute	14,500
4	Plant Unloading at 5% of Full Power per Minute	14,500
5	Step Load Increase of 10% of Full Power	2,000
6	Step Load Decrease of 10% of Full Power	2,000
7	Large Step Load Decrease with Steam Dump	200
8	Steady-state Fluctuations	
	Initial Fluctuations	1.5×10^5
	Random Fluctuations	3.0×10^6
9	Feedwater Cycling at Hot Standby	2,000
Upset Condition		
1	Loss of Load	80
2	Loss of AC Power	40
3	Loss of Flow	80
4	Reactor Trip	400
5	Inadvertent Auxiliary Spray	10
Faulted Conditions		
1	Loss of Coolant Accident[1]	1
2	Steam Line Break	1
Test Conditions		
1	Turbine Roll Test	10
2	Primary Side Hydrostatic Test	
	Initial Hydrostatic Test to 3,107 psig	1
	Subsequent Hydrostatic Test to 2,485 psig	5
3	Secondary Side Hydrostatic Test	
	Initial Hydrostatic Test to 1,356 psig	10
	Subsequent Hydrostatic Test to 1,085 psig	50
4	Primary-to-Secondary Side Leak Test to 2,435 psig	150
5	Primary-to-Secondary Side Leak Test to 2,250 psig	15
6	Secondary-to-Primary Side Leak Test to 840 psig	15

Note:

1. **Leak before break has been applied on the primary loop piping; therefore, the loss of coolant accident transient is not considered.**

Table 2-2 MOP I/O Transient Cycles per [8]

Heatup or Cooldown	Number of Events	Number of I/O Pairs per Event	Transient Name	ΔT	Percent of Total Events at This ΔT	Cycles
Heatup	200	2	IO_a	[		] a, c, e
			IO_b			
			IO_c			
			IO_d			
Cooldown	200	2	IO_a			
			IO_b			
			IO_c			
			IO_d			

Note: Since the I/O transients of the same ΔT are identical for heatup and cooldown, the cycles are combined to be:

- [ ] a, c, e

[ ] a, c, e

Figure 2-1 MOP Design Transient Time/Temperature Distribution Curve [8]

3 FINITE ELEMENT ANALYSIS

A three-dimensional finite element model (FEM) of the pressurizer lower head at the heater sleeve penetration region was created to determine the through-wall time history stresses. The model included the pressurizer lower head, heater sleeve penetration nozzle, cladding, and attachment weld. The detail finite element analysis is performed in [16].

3.1 METHOD DISCUSSION

A FEM was created in *ANSYS*®[1] with the assistance of computer-aided design (CAD) software and the ANSYS Workbench platform. Specifically, drawings [9] were used to make a three-dimensional section of the lower pressurizer head (see Figure 3-1) in SolidWorks. This section is a 5.14° [9b)] wedge of the head; 5.14° is half the angle between the outermost heater well assemblies. The CAD model is then imported as a para-solid into ANSYS Workbench to create additional geometric features for meshing purposes, and exported as an ANSYS neutral file for meshing in ANSYS Mechanical (Classic). ANSYS Mechanical is used for all meshing and analysis. FEM cut paths for outputting stress and temperature are illustrated in Figure 3-8 and Figure 3-9.

Fluid temperatures for the analyzed transients are applied to the wetted areas, excluding the inside of the thermal wells (see Figure 3-2). The inside of the thermal well is excluded because it is more appropriately modeled as adiabatic rather than convective. The thermal model with the boundary conditions (Section 3.4) was solved to obtain thermal distributions due to transients. Thermal distributions and transient pressure (including blowoff loads) are applied to the structural model to generate stress results at chosen time points for each transient. Thermal runs are solved as a transient analysis; structural runs are solved as a series of static steps.

There are three radial rows heaters [9a)], and the failed heater, #11, is on the inner row. However, the stresses for the outermost nozzle penetrations (#47 to #78) are typically more limiting due to the non-symmetrical geometry. This is consistent with previous analyses of similar geometry [18]. The FEM includes a representation of one outer heater well and one inner heater well assembly. Although the outermost heater location is considered to be limiting, stresses for both outermost and innermost wells are considered in the FEM.

[1] ANSYS, ANSYS Workbench, Ansoft, AUTODYN, CFX, EKM, Engineering Knowledge Manager, FLUENT, HFSS and any and all ANSYS, Inc. brand, product, service and feature names, logos and slogans are trademarks or registered trademarks of ANSYS, Inc. or its subsidiaries located in the United States or other countries. ICEM CFD is a trademark used by ANSYS, Inc. under license. CFX is a trademark of Sony Corporation in Japan. All other brand, product, service and feature names or trademarks are the property of their respective owners.

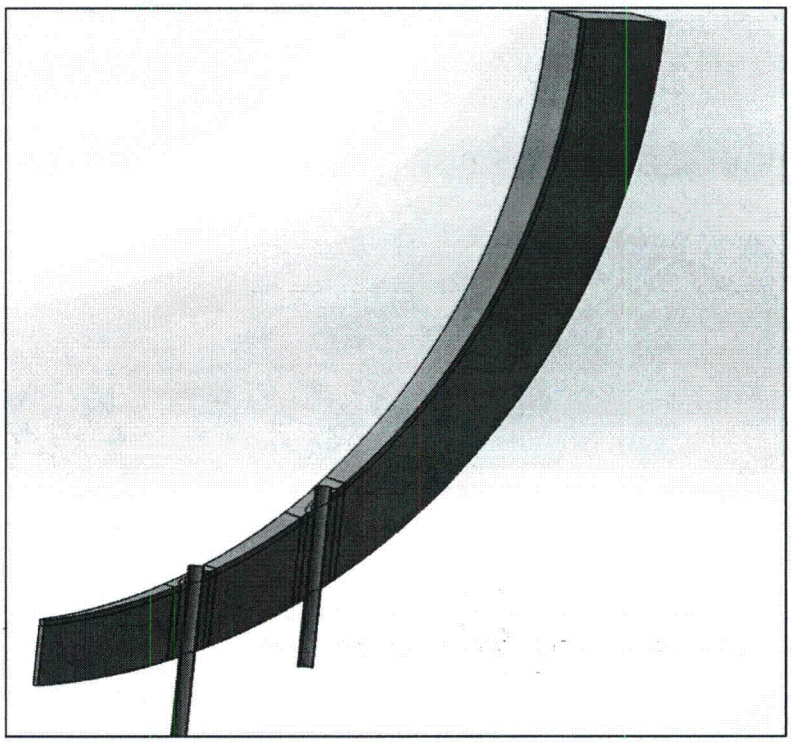

Figure 3-1 SolidWorks CAD Model

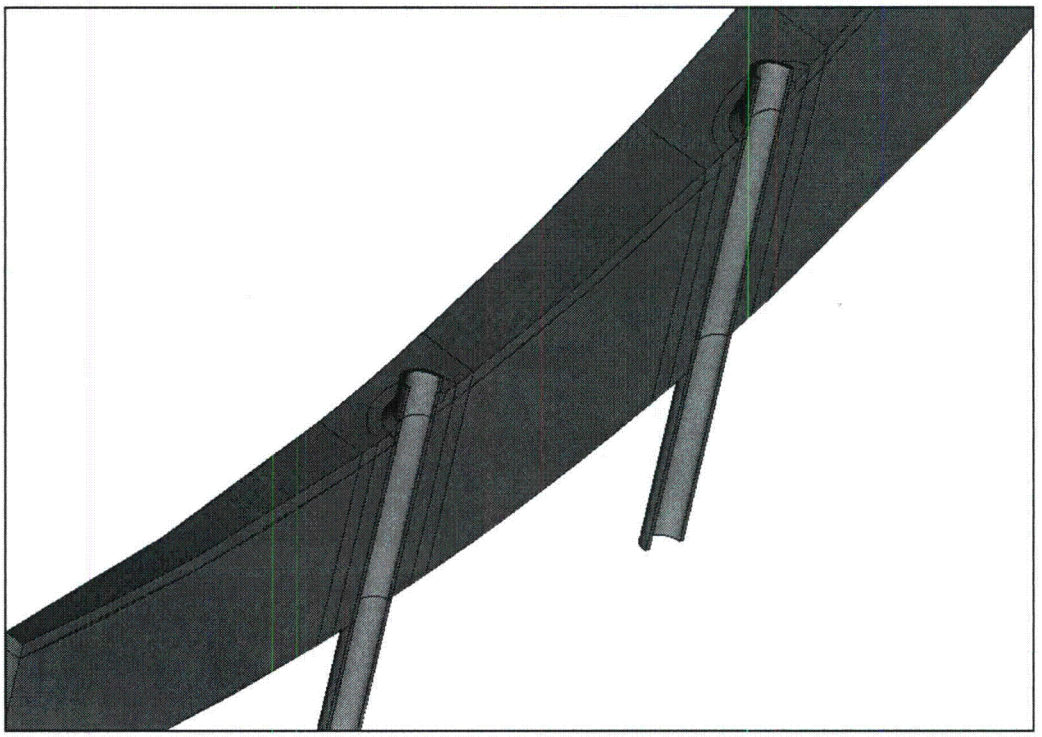

Figure 3-2 Wetted Area (Shown in Red)

3.2 MESHED MODEL

The FEM consists of all solid elements, a combination of 20-node bricks and 10-node tetrahedrons; mesh details are shown in Figure 3-3 through Figure 3-5. There are two versions of this FEM. The thermal version of the FEM consists of SOLID90 and SOLID87 elements; the structural model consists of SOLID186 and SOLID187 elements. Meshing and numbering are identical between the two versions.

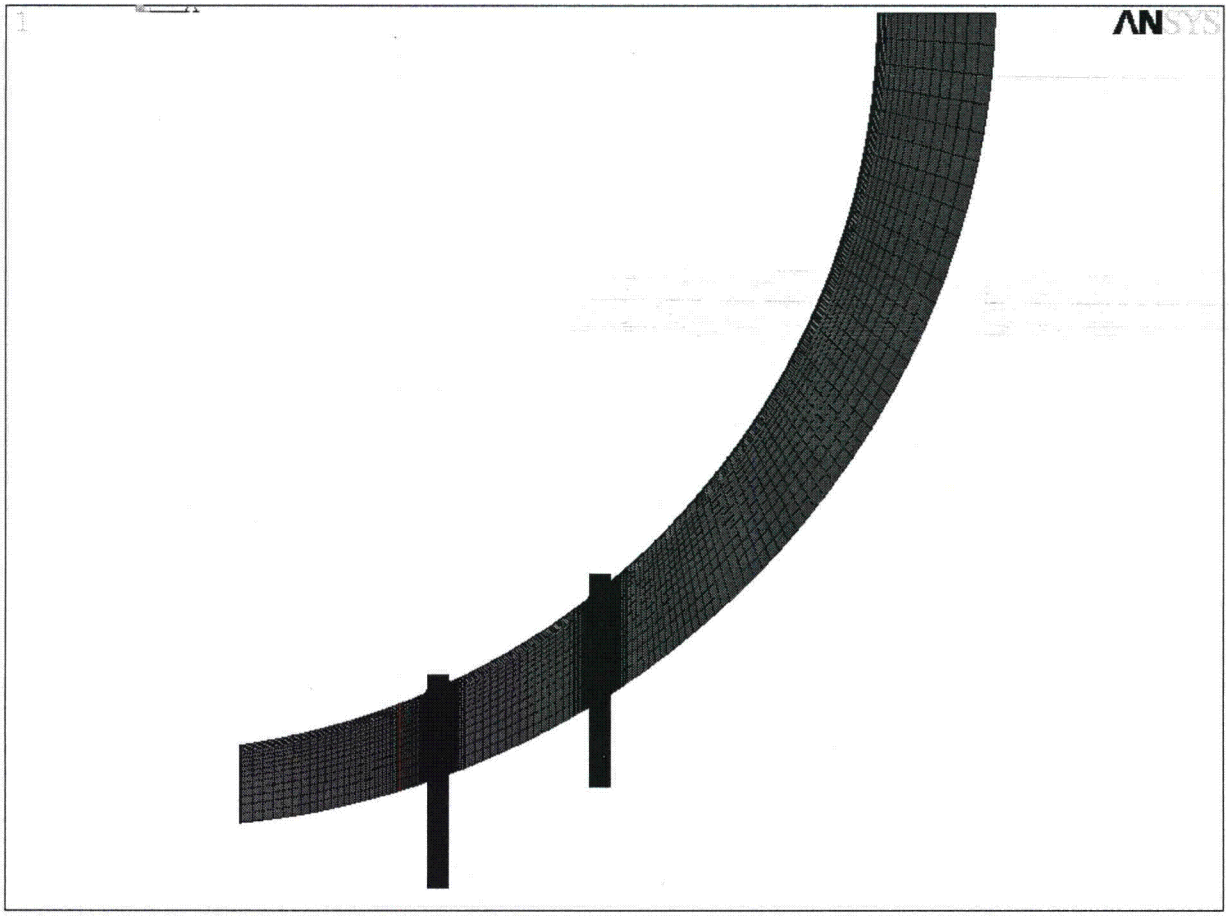

Figure 3-3 FEM Mesh

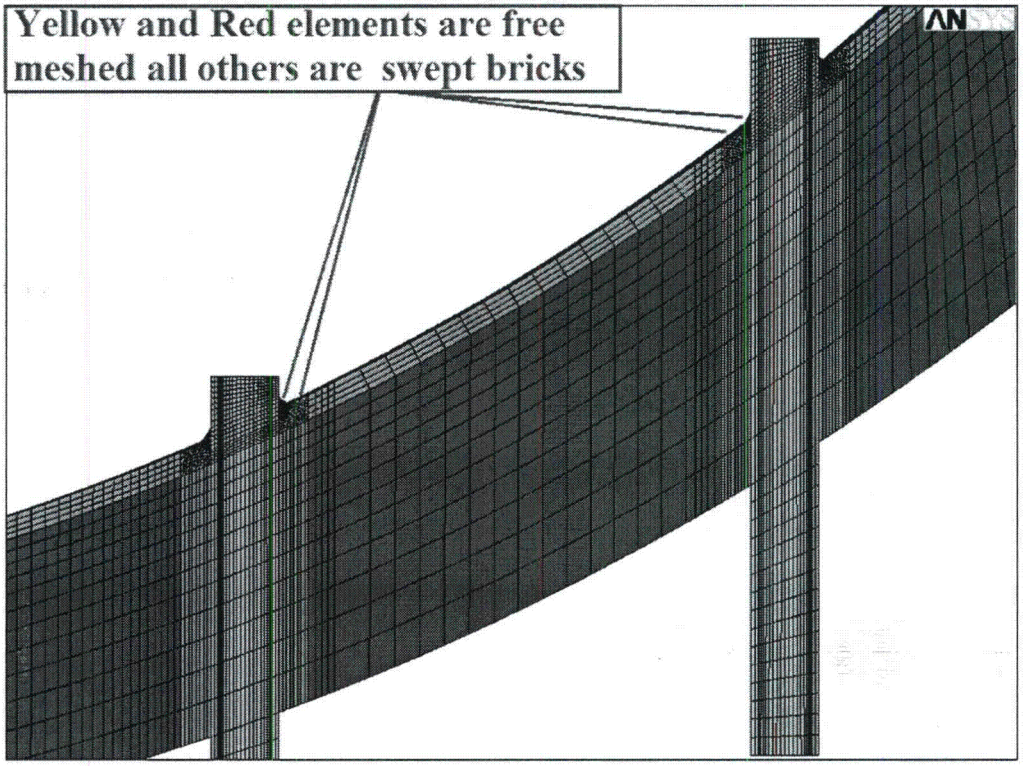

Figure 3-4 Heater Well FEM Mesh Detail

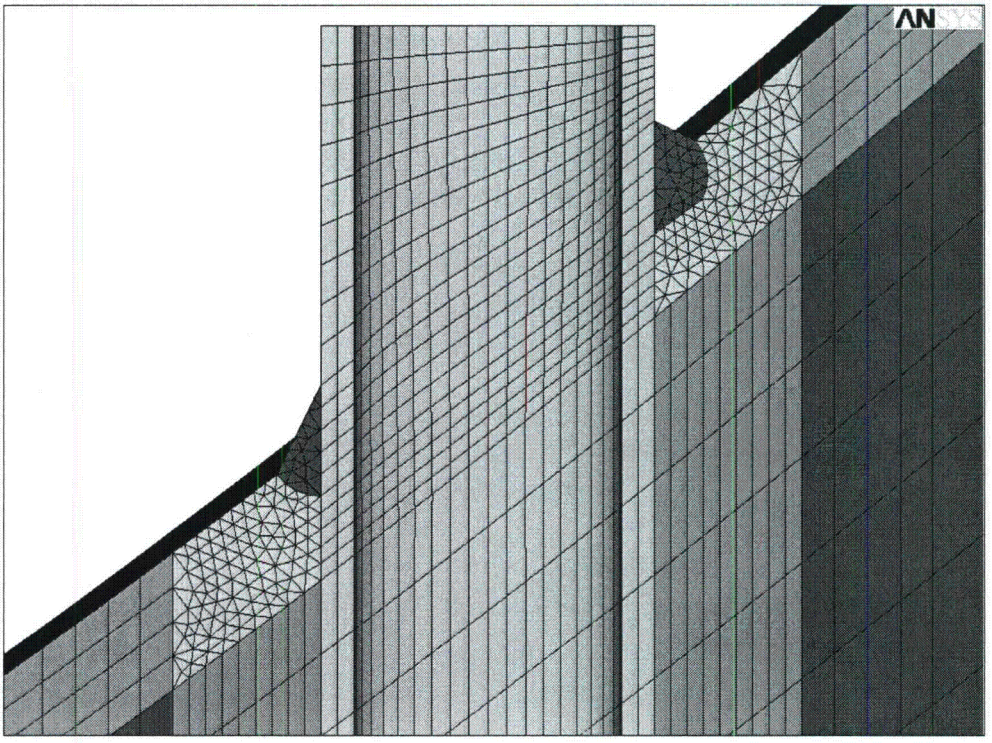

Figure 3-5 Outermost Heater Well Mesh Detail

3.3 FEM MATERIAL

The materials for the model are listed in Table 3-1.

Table 3-1 FEM Materials

Component	Material	Reference
Cladding	ER 308 and 309	9b)
Partial Penetration Weld	ER 308	9b)
Heater Well Assembly	SA-213 TP316	9d)
Pressurizer Lower Head	SA-216 Grade WCC	9c)

Note:

(1) ER308 and 309 are similar to 304 series stainless steel. For the purpose of this evaluation, it is assumed to be identical to SA-213, TP316.

3.4 BOUNDARY CONDITIONS

As discussed in Section 3.1, the FEM is a small wedge of the head. Symmetry planes are used on both sides of the wedge to simulate the full head. In the thermal runs, the outer diameter of the heater well is thermally coupled to coincident nodes on the head because the gap is assumed to be closed. In the structural runs, these nodes are coupled horizontally as illustrated in Figure 3-7. In the vertical direction, they are left free, conservatively allowing all vertical loads to pass through the partial penetration weld. As illustrated in Figure 3-6 the plane at the top of the head is fixed in the vertical y-direction and the bottom of each heater well is coupled vertically to eliminate erroneous distortion. Symmetry boundary conditions are applied to both sides of the wedge.

Per [10] and [11], a heat transfer coefficient of 200 BTU/hr-ft^2-°F applied to the wetted area is appropriate for all transients; see Figure 3-2. All other surfaces are assumed to be adiabatic. Transient pressure is applied to the wetted area, including the inside of the heater wells. Additionally, pressure is applied to the bottom of the thermal wells to account for blowoff loads.

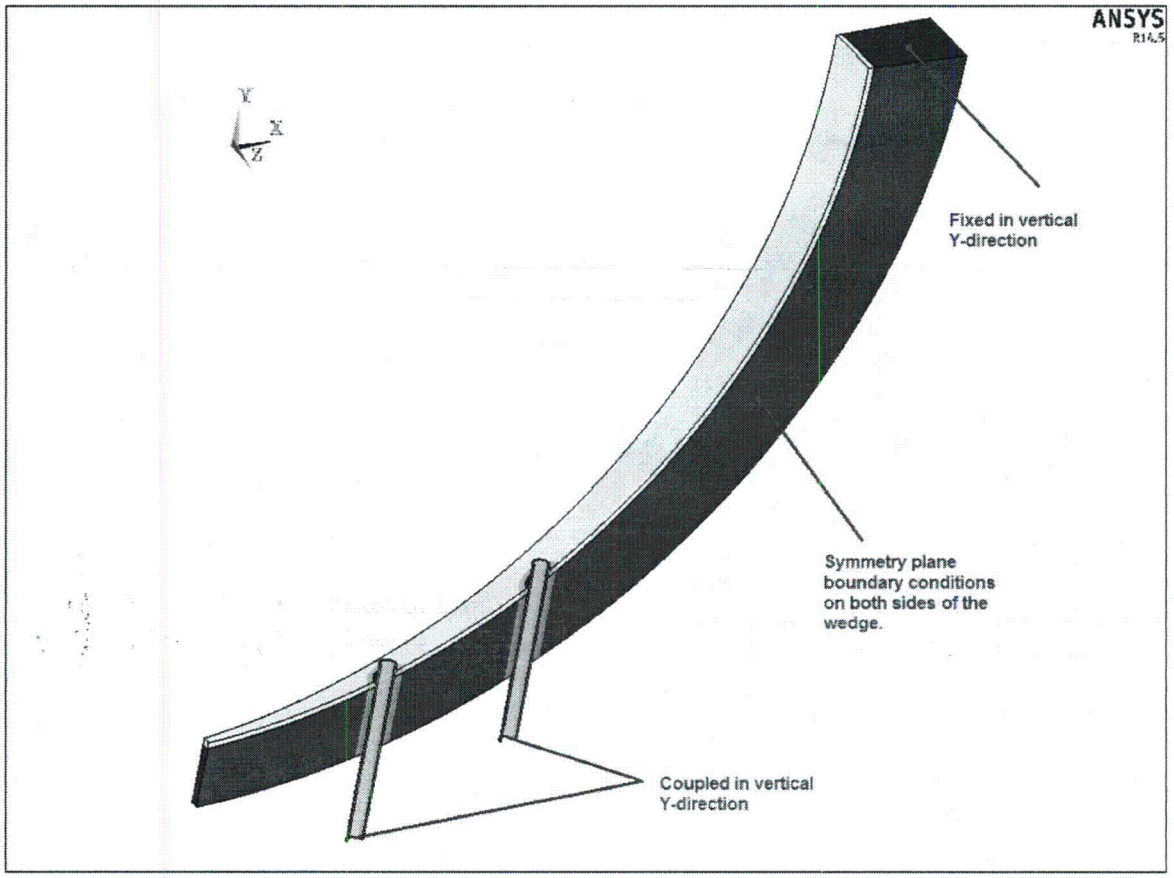

Figure 3-6 FEM Boundary Conditions

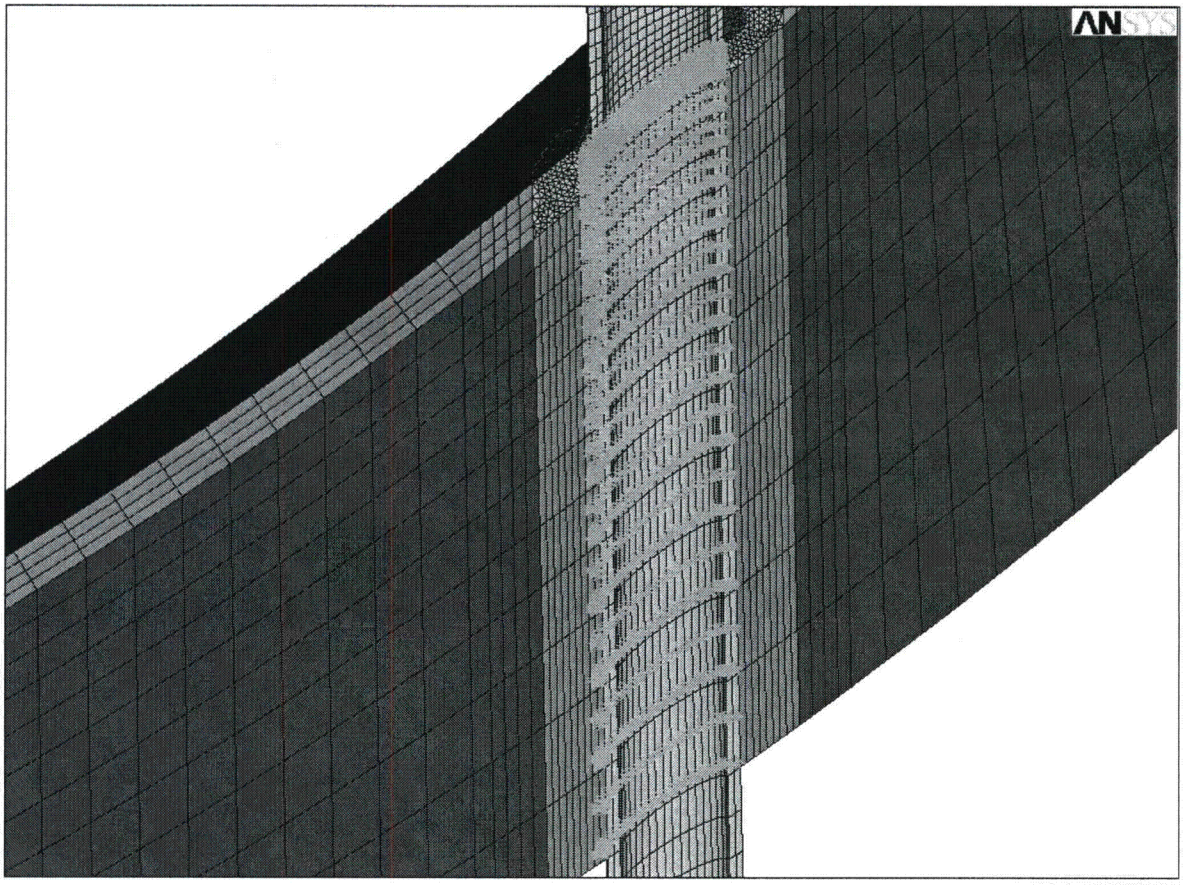

Figure 3-7 Heater Well Coupling to Head

3.5 PATH LOCATIONS

Results for cladding paths numbered 1 through 8 are outputted with 7 evenly spaced through-wall locations; the head paths numbered 9 through 16 are outputted with 16 through-wall locations. The location of each path is shown in Figure 3-8 and Figure 3-9.

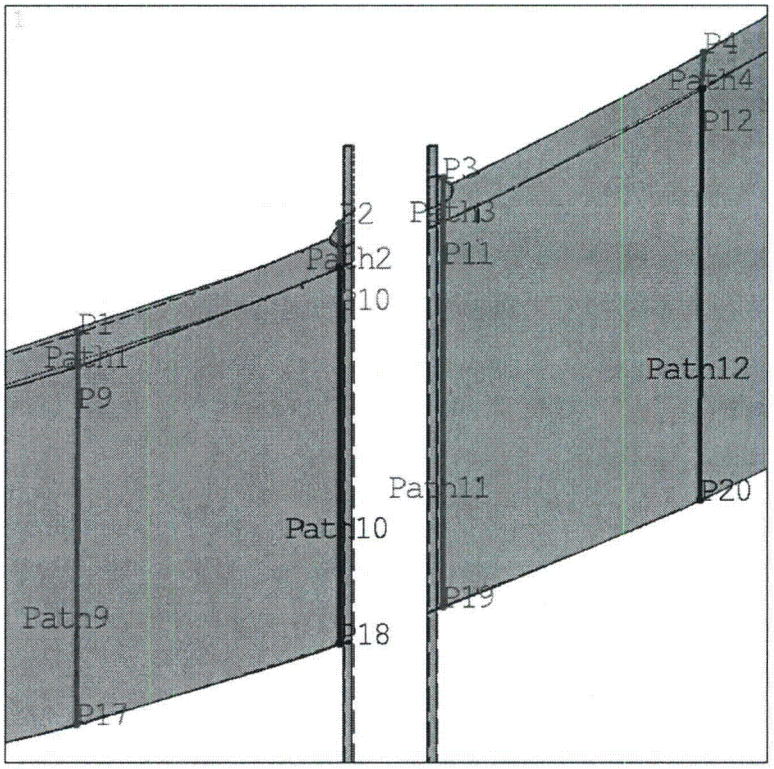

Figure 3-8 Innermost Heater Penetration Cut Paths

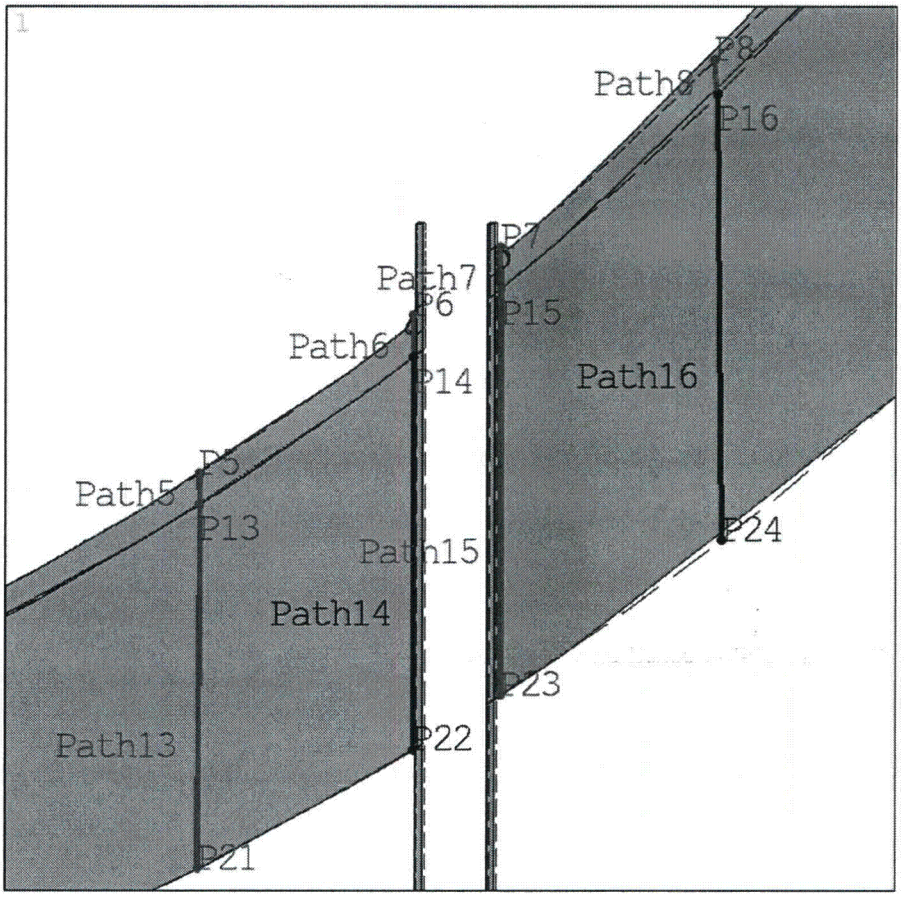

Figure 3-9 Outermost Heater Penetration Cut Paths

3.6 FEA RESULTS

Thermal results are post-processed to obtain through-wall temperature distributions for each transient at all chosen time points and sub-steps. These through-wall distributions are reviewed to ensure enough time points were chosen to capture the significant through-wall gradients throughout the transients.

Stresses and temperatures are output in the local coordinate system for each path (the positive x-direction is from the inside node of the path to the outside node, the positive y-direction is orthogonal and pointing away from the surge nozzle in the symmetry plane, and the z-direction is the cross product of x and y); see Figure 3-10.

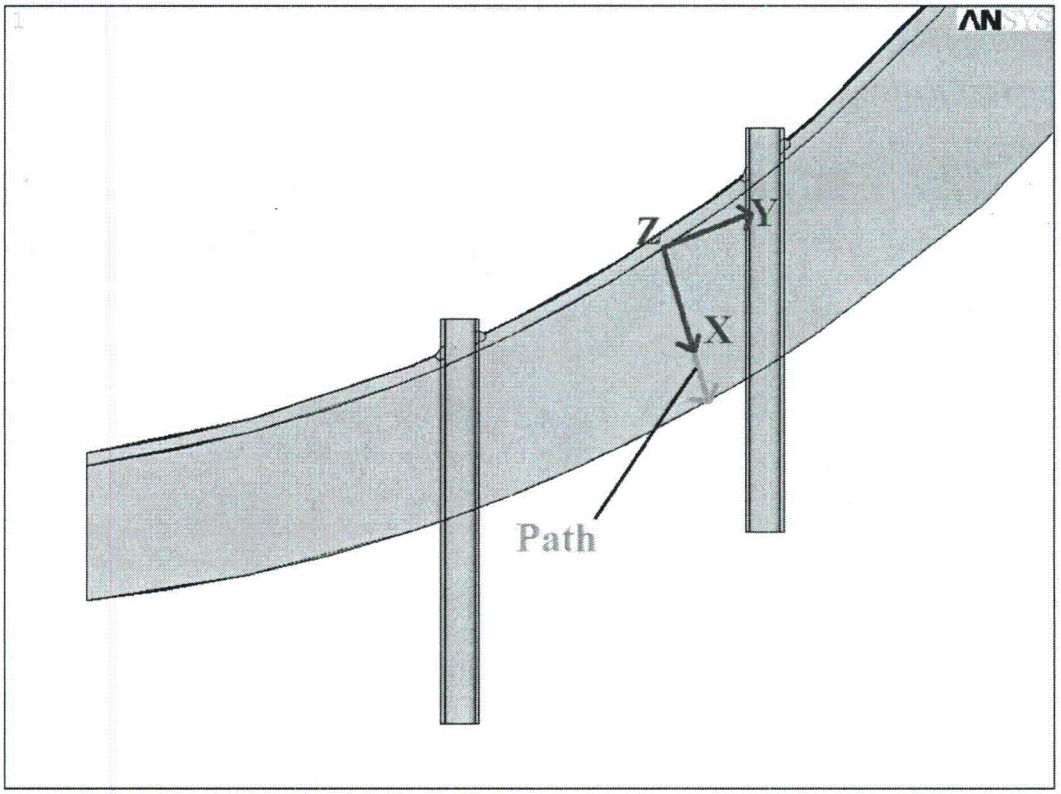

Figure 3-10 Local Path Coordinate System

Note: The sample path line shown in Figure 3-10 is for illustration purposes to show the local result coordinate system.

4 FRACTURE MECHANICS EVALUATION

To support continued operation of Turkey Point Units 3 and 4 with a half-nozzle repair to a heater sleeve, a fracture mechanics evaluation is performed in accordance with the ASME Section XI IWB-3600 in-service inspection evaluation procedure and acceptance criteria [1]. The key aspect of the fracture mechanics analysis is to demonstrate the structural integrity of the pressurizer lower head with a flawed heater sleeve partial penetration attachment weld. A crack growth chart is generated for the pressurizer lower head to demonstrate that the growth of a flaw postulated in the heater sleeve partial penetration weld through the pressurizer lower head base material remains within acceptable limits. The final flaw size after a selected operation duration of interest can then be compared to the maximum allowable end-of-evaluation period flaw size defined based on an ASME Section XI flaw stability analysis. The detailed fracture mechanics analysis is performed in [17].

4.1 METHODOLOGY

In order to demonstrate acceptability of an indication for future plant operation, the maximum allowable end-of-evaluation period flaw sizes at the location of interest are first determined. The maximum allowable end-of-evaluation period flaw size is the largest flaw that can exist in the component without violating the acceptance criteria set forth by the ASME Section XI Code. The maximum allowable end-of-evaluation period flaw sizes are determined in accordance with the in-service inspection evaluation procedure shown in ASME Section XI paragraph IWB-3610 based on through-wall operating pressure and thermal transient stresses, crack geometry, and material properties. Crack growth evaluations are then performed based on a postulated initial flaw to determine the growth as a function of operation duration. The initial flaw is postulated with a depth equal to the partial penetration weld plus cladding thickness; thus, the deepest extent of the flaw will reach the inside surface of the pressurizer lower head base material. The final flaw size based on the crack growth analysis at the end of an operation duration can then be compared to the maximum allowable end-of-evaluation period flaw size to determine acceptability for future service. The heater penetrations are sufficiently far away from one another that the flaws in adjacent penetration locations will not coalesce to provide a more limiting result than that already concluded in Section 5 of this report. Evaluations will be completed for multiple path locations (See Figure 3-8 and Figure 3-9) at the heater sleeve penetration, and the most limiting results will be used to demonstrate flaw stability.

4.1.1 Pressure/Thermal Transient Stresses

In determining the maximum allowable end-of-evaluation period flaw sizes based on the acceptance criteria in IWB-3600 and fatigue crack growth, it is essential that all applicable loadings be considered. The first step of the evaluation is to determine the transient loading at the location of interest and, therefore, all the applicable pressure/thermal transients for the normal/upset/test and emergency/faulted conditions must be considered. The applicable pressure/thermal transients and the corresponding transient cycles during the design life of the pressurizer are discussed in Section 2. The corresponding design temperature and pressure transient curves are used in developing the time history through-wall pressure/thermal transient stress which is used as input to the fracture mechanics evaluation.

Transient stresses are determined based on the finite element analysis determined in Section 3, which modeled the area of interest in the pressurizer lower head. The model included the lower head base metal, penetration nozzle, attachment weld, and the cladding. The transient stresses used in the flaw evaluation are based on the outermost row of heater penetrations because the stresses in this row are the highest of all the penetrations. The differences in the transient stress results between the outermost row of penetrations and the innermost row are insignificant. Therefore, use of the transient stresses for the outermost penetration nozzle is appropriate for enveloping all heater sleeve penetrations in the pressurizer lower head.

The outer penetration model contains four total paths, along which transient stresses are determined, that extend from the inside surface of the cladding to the outside surface of the base metal, as shown in Figure 3-9. Two paths are on the downhill side of the penetration (Paths 5/13 and 6/14), and two paths are on the uphill side of the penetration (Paths 8/16 and 7/15), as shown in Figure 3-9. Although the stress intensity factor definition from [12] calls for remote stresses to be used, Paths 6/14 and 7/15 are used in the evaluation since they produce more limiting stresses and conservative results.

4.1.2 Crack Tip Stress Intensity Factors

One of the key elements in determining the maximum allowable flaw size and the fatigue crack growth is the stress intensity factor (K_I) or the driving force on the crack. This is determined using expressions available from the public literature. In all cases, the crack tip stress intensity factor calculations utilized a linear representation of the actual through-wall stress profile. The model used to evaluate the postulated flaws in the attachment weld is two corner flaws which extend radially into the pressurizer lower head (Figure 4-1). The details of the postulated crack are shown in Figure 4-2.

The stress intensity factor expression for two corner flaws emanating from the edge of a hole in a plate [12] was used in determining the stress intensity factor for the postulated flaw in the partial penetration weld (Figure 4-2). The stress intensity factor can be expressed in terms of the membrane and bending stress components as follows:

$$K_I = (M_m (\sigma_m + p_c) + M_b \sigma_b) (\pi a/Q)^{1/2}$$

Where,

σ_m = remote membrane stress component
σ_b = remote bending stress component
p_c = crack face pressure (2.25 ksi)
M_m = boundary correction factor for remote membrane [12]
M_b = boundary correction factor for remote bending [12]
Q = shape factor per [12]
a = depth of the corner flaw

Use of this method requires that the stresses remote from the hole be resolved into membrane and bending stress components.

The expression in [12] is applicable for a range of flaw shapes, with the depth of the flaw defined as "a" and the width of the flaw defined as "c", as shown in Figure 4-1. The attachment weld dimensions were based on the partial penetration weld geometry, which is shown in Figure 3-5. It should be noted that there is an additional layer of cladding between the partial penetration weld and the pressurizer lower head. This additional layer of cladding is conservatively assumed to be flawed, thus, the initial flaw depth includes the depth of both layers of cladding.

M_m and M_b are determined based on the transient stress evaluation discussed in Section 3 for the plant-specific geometry (R/t) and flaw shape (a/c) ratios and various a/t and $2\phi/\pi$ ratios. R is the radius of the hole, t is the thickness of the pressurizer head, and ϕ is the angular position of a point on the crack front (see Figure 4-1).

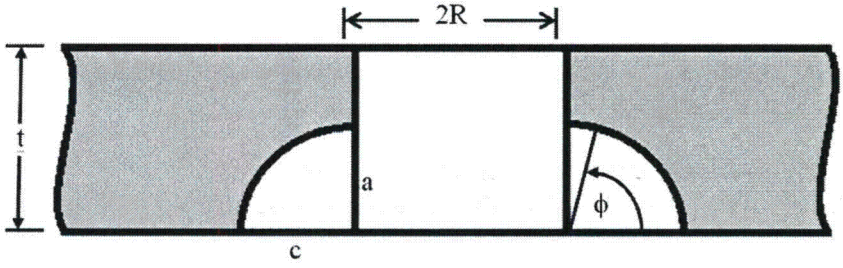

Figure 4-1 Corner Crack Geometry [12]

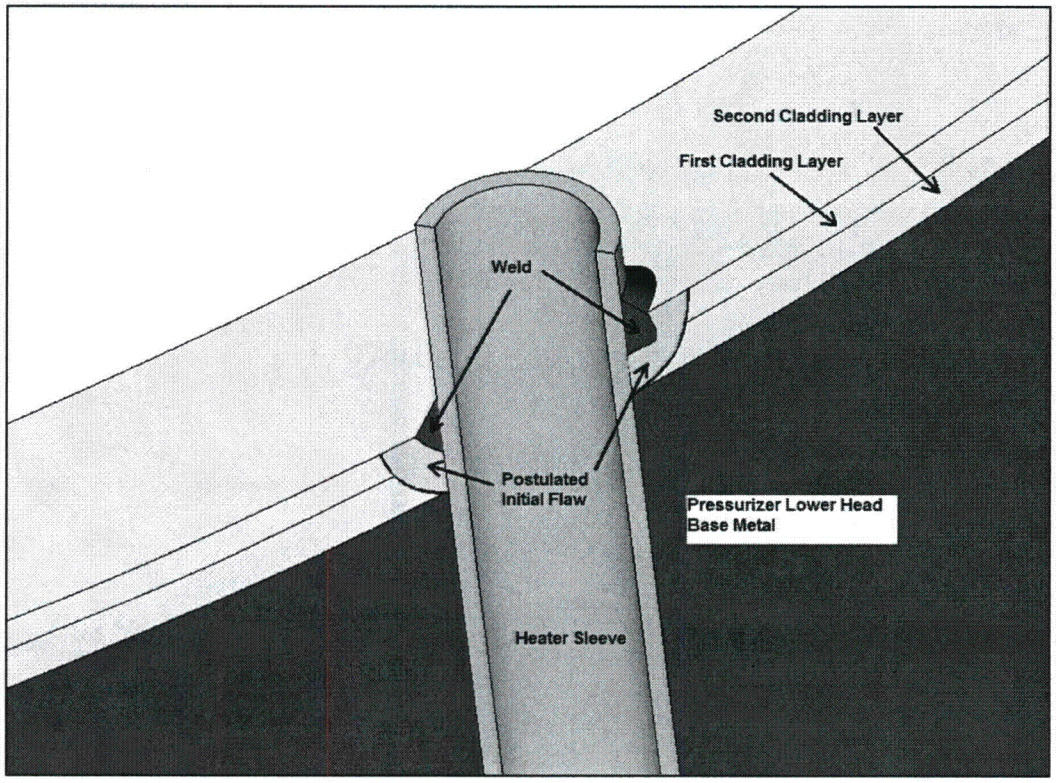

Figure 4-2 Initial Flaw Postulated at the Heater Sleeve Attachment Weld

4.2 MAXIMUM ALLOWABLE END-OF-EVALUATION PERIOD FLAW SIZE DETERMINATION

In order to demonstrate acceptability of the postulated indication for future plant operation, the maximum allowable end-of-evaluation period flaw sizes at the location of interest are first determined based on ASME Section XI, IWB-3600. The crack growth based on operation duration is then calculated and compared to the maximum allowable end-of-evaluation period flaw sizes to determine acceptability of the postulated initial flaw for future service. The following sections provide a discussion of the maximum allowable end-of-evaluation period flaw size determination.

4.2.1 ASME Section XI Flaw Size Acceptance Criteria

There are two alternative sets of flaw acceptance criteria for continued service without repair in paragraph IWB-3600 of the ASME Section XI Code. Either of the criteria below may be used per paragraph IWB-3610 to determine the maximum allowable end-of-evaluation period flaw size.

1. Acceptance Criteria Based on Flaw Size (IWB-3611)
2. Acceptance Criteria Based on Stress Intensity Factor (IWB-3612)

In addition to the above two acceptance criteria, paragraph IWB-3610 of the ASME Section XI Code also requires that the primary stress limit of ASME Section III NB-3000 be met assuming a local area reduction of the pressure retaining membrane that is equal to the area of the flaw. Therefore, the maximum allowable flaw size determined using the primary stress limit is also used in the maximum allowable end-of-evaluation period flaw size determination.

4.2.1.1 Acceptance Criteria Based on Flaw Size

The acceptance criteria based on flaw size as stated in IWB-3611 of ASME Section XI are:

$a_f < 0.1\ a_c$ for normal conditions (including upset and test conditions)

$a_f < 0.5\ a_i$ for emergency/faulted conditions

Where,

a_f = the maximum size to which the flaw is calculated to grow to at the end of a specific period (maximum allowable end-of-evaluation period flaw size).

a_c = the minimum critical flaw size under normal operating conditions (upset and test conditions inclusive).

a_i = the minimum critical flaw size for initiation of non-arresting growth under postulated emergency and faulted conditions.

To determine whether an indication is acceptable for continued service without repair, the acceptance criteria for both normal and emergency/faulted conditions must be met and only the

most restrictive results from these service conditions are used in determining the maximum allowable flaw size based on the flaw size acceptance criteria.

The flaw size acceptance criteria used to determine the maximum allowable end-of-evaluation period flaw size for the normal (upset and test inclusive) and emergency/faulted transients are further determined based on the methodology in Appendix A-5000 of the Section XI ASME Code. For all normal/upset/test condition transients, the critical flaw size, a_c, corresponding to fracture initiation (e.g., K_{Ic}) is determined.

For all emergency/faulted condition transients, the flaw size, a_c, at fracture initiation (e.g., K_{Ic}) and the flaw size, a_a, at fracture arrest (e.g., K_{Ia}) are determined. When the flaw size at fracture arrest (denoted as a_a) is greater than 75% of the wall thickness, the fracture initiation flaw size is used to represent a_i. If the flaw arrests before reaching 75% of wall thickness, the critical flaw size is 1.0. If the flaw does not arrest but initiates, the critical flaw size is flaw size at initiation a_c.

The fracture toughness for ferritic steel has been taken directly from the reference curves of Appendix A in the ASME Section XI Code. In the transition temperature region, these curves can be represented by the following equations:

$$K_{Ic} = 33.2 + 20.734\exp[0.02\ (T\text{-}RT_{NDT})]$$

$$K_{Ia} = 26.8 + 12.445\exp[0.0145\ (T\text{-}RT_{NDT})]$$

Where K_{Ic} and K_{Ia} are in ksi$\sqrt{in}$, T and RT_{NDT} are as follows:

T = crack tip temperature (°F)

RT_{NDT} = reference temperature for nil ductility transition (°F)

One of the key inputs required in the determination of the fracture toughness for ferritic steel is the value of RT_{NDT}, which is a parameter determined from the Charpy V-notch and drop-weight tests. The lower head is made of cast steel, SA-216-WCC. A compilation of fracture toughness for this steel is shown in Figure 4-3 [15], along with the ASME Section XI K_{IC} curve, with an assumed RT_{NDT} = [ ]^{a,c,e}. Therefore, the initial unirradiated RT_{NDT} value used for the Turkey Point Units 3 and 4 pressurizer lower head material is [ ]^{a,c,e} and can be used in determining the fracture toughness since, at the location of interest, the RT_{NDT} is not affected by the service life and condition. The upper shelf temperature regime requires utilization of a shelf toughness which is not specified in the ASME Code. A maximum value of 200 ksi$\sqrt{in}$ is used since it is consistent with general practice in such evaluations [13], which provides the background and technical basis of Appendix A of the ASME Section XI Code.

a,c,e

Figure 4-3 A216 Gr. WCC Fracture Toughness, K_{IC} [15]

4.2.1.2 Acceptance Criteria Based on Stress Intensity Factor

The term stress intensity factor (K_I) is defined as the driving force on a crack. It is a function of the size of the crack and the applied stresses, as well as the overall geometry of the structure. In contrast, the fracture toughness (K_{Ic}) is a measure of the resistance of the material to crack propagation. The acceptance criteria based on the crack tip stress intensity factor as stated in IWB-3612 of ASME Section XI [1] are:

$$K_I < \frac{K_{Ic}}{\sqrt{10}} \text{ for normal conditions (upset and test conditions inclusive)}$$

$$K_I < \frac{K_{Ic}}{\sqrt{2}} \text{ for emergency/faulted conditions}$$

Where,

K_I = maximum applied stress intensity factor for flaw size a_f to which a flaw will grow, during the conditions under consideration, for a specified period, or to the next inspection.

K_{Ic} = fracture toughness based on fracture initiation for the corresponding crack tip temperature.

To determine whether an indication is acceptable for continued service without repair, the acceptance criteria for both normal and emergency/faulted conditions must be met and only the

most restrictive results from these two sets of service conditions are used in determining the maximum allowable flaw size based on the stress intensity factor acceptance criteria.

In determining the maximum allowable end-of-evaluation period flaw size for the location of interest, the acceptance criteria based on the flaw size and crack tip stress intensity factor discussed above are used. An evaluation is first performed using the flaw size acceptance criteria to determine the smallest allowable flaw size for all applicable design transients. A second evaluation is then performed using the criteria based on the stress intensity factor to determine the smallest allowable flaw size for all applicable design transients. The results from the two evaluations are then compared and the largest allowable flaw size is determined. The largest allowable flaw size determined based on Sections 4.2.1.1 and 4.2.1.2 is then compared to the primary stress limit calculation and the smallest value is used as the maximum allowable end-of-evaluation period flaw size for the location of interest.

4.2.1.3 Primary Stress Limit

In addition to satisfying the above acceptance criteria, paragraph IWB-3610 requires that the primary stress limits of the ASME Code Section III, Article NB-3000 be satisfied assuming a local area reduction of the pressure retaining membrane that is equal to the area of the indication. The maximum flaw size allowed based on the primary stress limit is compared to those found using the flaw size and stress intensity factor acceptance criteria and the most limiting is used as the maximum allowable end-of-evaluation period flaw size.

4.3 CRACK GROWTH EVALUATION

Once the maximum allowable end-of-evaluation period flaw sizes are determined, a crack growth evaluation is performed using fatigue and corrosion crack growth mechanisms. The crack growth evaluation is used to construct the crack growth chart. The crack growth chart can then be used with the maximum allowable end-of-evaluation period flaw sizes to determine allowable service life.

The crack growth analysis procedure involves postulating an initial flaw at the location of interest and calculating the crack growth due to design pressure/thermal transients and corrosion. The input required for the fatigue crack growth portion of the analysis is basically the information necessary to calculate the crack tip stress intensity factor range (ΔK_I, see Section 4.3.2), which depends on the geometry of the crack, its surrounding structure, and the range of applied stresses in the area of interest. Once ΔK_I is calculated, the growth due to a particular transient stress cycle can be calculated using the applicable fatigue crack growth reference curves for ferritic steel in Appendix A of the ASME Section XI Code. This incremental growth is then added to the original crack size with the flaw aspect ratio remaining constant, and the analysis proceeds to the next cycle or transient. The procedure is continued in this manner until all of the applicable pressure/thermal transients for the design life of the plant have been analyzed.

The through-wall normal, upset, and test condition pressures and thermal transient stresses at the location of interest due to plant-specific pressure and thermal transients, as well as the associated design transient cycles, are used as input for the generation of crack growth chart. The chart is generated in accordance with the 2007 Edition with 2008 Addenda ASME Code [1].

The following sections provide a more detailed discussion of the methodology used in the ASME Section XI flaw growth evaluation.

4.3.1 Corrosion Growth

A corrosion crack growth study for pressurizer low alloy steel has been performed to support small-diameter half-nozzle repair and replacement programs in WCAP-15973-P-A [14]. These half-nozzle repairs are unique in that high oxygen levels may be present in the crevice between the heater sleeve nozzles and the pressurizer base material during start-up from refueling and other outages when the primary system is open. During the time when the plant returns to operation from a shutdown condition (i.e., refueling), the crevice region may be filled with aerated water. The oxygen in the water will be consumed by corrosion of the steel; however, the corrosion rate will be high for the relatively short time when the temperature is at a low to moderate level. When the plant is operating, the crevice region will be de-aerated, and the corrosion rate is much less than that during the time immediately after startup.

The corrosion crack growth study determined the corrosion rate during three separate operating conditions; full power operation, startup mode (assumed to be at intermediate temperature with aerated primary coolant), and refueling mode (100°F with aerated primary coolant). Corrosion rates of [ ]^{a,c,e} mils per year were assumed for full power operation, startup mode, and refueling mode, respectively, based on WCAP-15973-P-A [14]. An overall corrosion rate is

then determined based on the corrosion rates of the individual operating modes and the expected percentage of time spent in each mode. For the purpose of this evaluation the plants are expected to operate at full power for [ ]^{a,c,e} of the time, startup conditions for [ ]^{a,c,e} of the time, and refueling conditions for [ ]^{a,c,e} of the time. Based on the individual operating condition corrosion rates and the expected percentage of time spent in each mode, an overall corrosion rate of [ ]^{a,c,e} mils per year was determined for the pressurizer base metal. In order to account for the possible corrosion of the Turkey Point Units 3 and 4 pressurizer lower head resulting from flawed heater sleeve partial penetration weld and flawed cladding, the same corrosion rate is assumed for the fracture mechanics evaluation contained herein. This corrosion rate was combined with the crack growth due to fatigue to calculate the total crack extension over time. It should be noted that the above mentioned corrosion rates are conservatively based on exposure to bulk primary coolant. However, when corrosion occurs in the crevice region between the pressurizer lower head and heater sleeve, the crevice will fill with corrosion products. The presence of these corrosion products will slow, or stifle, the corrosion process because bulk primary coolant access to the base metal will be restricted. Nevertheless, the full corrosion rates from WCAP-15973-P-A are conservatively utilized herein.

An additional evaluation, independent of the original design evaluation, was performed to determine the acceptable life of the repair weld that is on the outside surface of the pressurizer lower head considering corrosion of the pressurizer lower head material. A similar evaluation was performed in Section 2.4 of WCAP-15973-P-A [14]. Corrosion of the pressurizer lower head material would increase the diameter of the heater sleeve bore, decreasing the area of the effective weld and the reinforcement area around the hole. The maximum allowable hole diameter is calculated considering the reduction in the effective weld shear area and the required area of reinforcement based on Section III of the ASME Code. The evaluation determined that a hole diameter increase of 0.435 inch is justifiable for the heater sleeve penetrations. Based on a corrosion rate of [ ]^{a,c,e} mils per year, it would take more than [ ]^{a,c,e} years for the hole diameter to increase by 0.435 inch. Since the remaining service lives of Turkey Point Units 3 and 4 are less than 40 years each, the heater sleeve hole diameter remains acceptable, even with corrosion, for the remaining life of the plants.

For the heater sleeve bore to reach the maximum allowable diameter within 20 years, a corrosion rate of approximately [ ]^{a,c,e} mils per year is required. A corrosion rate of [ ]^{a,c,e} mils per year corresponds to a time split of [ ]^{a,c,e} of the time at the operating condition ([ ]^{a,c,e} mils per year corrosion rate) and [ ]^{a,c,e} of the time at the startup condition ([ ]^{a,c,e} mils per year corrosion rate). For the heater sleeve bore to reach the maximum allowable diameter within 40 years, a corrosion rate of approximately [ ]^{a,c,e} mils per year is required, which corresponds to a time split of [ ]^{a,c,e} of the time at the operating condition ([ ]^{a,c,e} mils per year corrosion rate) and [ ]^{a,c,e} of the time at the startup condition ([ ]^{a,c,e} mils per year corrosion rate). These values were conservatively determined using only operating condition and startup condition corrosion rates based on WCAP-15973-P. The corrosion rate at the startup condition is more conservative than the corrosion rate at the refueling condition. Any time spent in the refueling mode would reduce the amount of time required at full power operation.

4.3.2 Fatigue Crack Growth Rate

The normal, test, and upset operating transients from Table 2-1 and Table 2-2 are considered in the fatigue crack growth analysis. The full amount of transient cycles shown in Table 2-1 and Table 2-2 is conservatively distributed equally over a plant life of 40 years. Using the total design cycles, the 40-year evaluation is conservative since Turkey Point Units 3 and 4 are approved for license renewal and have already operated for more than 40 years. The crack growth rate curves used for the ferritic steel reactor vessel material are taken directly from Article A-4000 in Appendix A of the ASME Section XI Code. The water environment curves are used since the analysis assumes the flaw encompasses the entire weld and has gone through the cladding. The initial crack tip is at the interface between the cladding and base metal.

The crack growth rate (da/dN) is a function of the applied stress intensity factor range (ΔK_I) and the R ratio (K_{min}/K_{max}) for the transient. The general form for fatigue crack growth is as follows based on ASME Section XI Appendix A [1]:

$$da/dN = C_o(\Delta K_I)^n$$

Where:

$$\Delta K_I = K_{max} - K_{min}$$

$$R = K_{min}/K_{max} \qquad (K_{min} > 0)$$

$$R = 0 \qquad (K_{min} \leq 0)$$

$$C_0 = 0 \text{ for } \Delta K_I < \Delta K_{th}$$

$$\Delta K_{th} = 5.0(1\text{-}0.8R)$$

According to Article A-4000 of the ASME Section XI Code, the limiting crack growth results based on using the n and C_0 values for fatigue crack growth in air from A-4300(b)(1) or those for water from A-4300(b)(2) should be used. The fatigue crack growth rates for both environments are discussed below.

Fatigue Crack Growth Rate for Air (ΔK_I values in ksi$\sqrt{in}$):

$$da/dN = 1.99 \times 10^{-10} (S)(\Delta K_I)^{3.07} \text{ in/cycle}$$

Where: $S = 25.72\ (2.88\text{-}R)^{-3.07}$

Fatigue Crack Growth Rate for Water (ΔK_I values in ksi$\sqrt{in}$):

$$\Delta K_{knee} = 17.74 \qquad (0 \leq R \leq 0.25)$$

$$\Delta K_{knee} = 17.74[(3.75\ R+0.06)/(26.9\ R\text{-}5.725)]^{0.25} \qquad (0.25 < R < 0.65)$$

$$\Delta K_{knee} = 12.04 \qquad (0.65 \leq R \leq 1.0)$$

For low ΔK_I values ($\Delta K_I < \Delta K_{knee}$):

$$da/dN = 1.02 \times 10^{-12} (S)(\Delta K_I)^{5.95} \text{ in/cycle}$$

Where:

$$\begin{aligned} S &= 1.0 && (0 \leq R \leq 0.25) \\ &= 26.9\,R - 5.725 && (0.25 < R < 0.65) \\ &= 11.76 && (0.65 \leq R \leq 1.0) \end{aligned}$$

For high ΔK_I values ($\Delta K_I > \Delta K_{knee}$):

$$da/dN = 1.01 \times 10^{-7} (S)(\Delta K_I)^{1.95} \text{ in/cycle}$$

Where:

$$\begin{aligned} S &= 1.0 && (0 \leq R \leq 0.25) \\ &= 3.75\,R + 0.06 && (0.25 < R < 0.65) \\ &= 2.5 && (0.65 \leq R \leq 1.0) \end{aligned}$$

4.4 FRACTURE MECHANICS RESULTS

4.4.1 Maximum Allowable End-of-Evaluation Period Flaw Size

All of the applicable design pressure/thermal transients are considered, and the governing transients are determined to be those which produced the most limiting allowable end-of-evaluation period flaw size. The maximum allowable end-of-evaluation period flaw sizes are determined based on the acceptance criteria in Section 4.2.1, which is based on Section XI of the ASME Code.

For the normal, upset, and test conditions, the maximum allowable end-of-evaluation period flaw sizes are based on the material fracture toughness values of K_{Ic} and the acceptance criteria in ASME Section XI Paragraphs IWB-3611 or IWB-3612. For the emergency and faulted conditions, the maximum allowable end-of-evaluation period flaw sizes are based on the material fracture toughness values of K_{Ic} and K_{Ia} and the acceptance criteria in ASME Section XI Paragraphs IWB-3611 or IWB-3612. It should be noted that upper shelf for fracture toughness is 200 ksi$\sqrt{in}$.

Maximum allowable end-of-evaluation period flaw sizes are determined in accordance with the methodology in IWB-3610 of the ASME Code. The stress intensity factors for all transients of interest are determined based on an aspect ratio, flaw length/flaw depth, or c/a = 1. For the evaluation contained herein, the attachment weld is assumed to be flawed, and the attachment weld has an aspect ratio of 1. The aspect ratio is conservatively assumed to remain constant as the flaw grows. Stress intensity factors are determined at both the deepest and surface point of the flaw. Stress profiles are used from Paths 6/14 and 7/15 shown in Figure 3-9, which correspond to the carbon steel pressurizer head at the outermost heater penetration.

The critical flaw sizes determined for the limiting normal, upset, and test condition transients are then compared to those of the most limiting emergency and faulted condition transients. Once the critical flaw sizes for normal/upset/test and emergency/faulted transients have been established, the limiting critical flaw sizes from all transient conditions are used to determine the maximum allowable end-of-evaluation period flaw sizes. The maximum allowable end-of-evaluation period flaw sizes are compared and the most limiting (smallest) flaw size for all operating conditions (normal/upset/test/emergency/faulted) is used as the final allowable flaw size in the crack growth calculation.

In addition to the critical flaw sizes for normal/upset/test and emergency/faulted transients, paragraph IWB-3610 of the ASME Section XI Code also requires that the primary stress limit of ASME Section III NB-3000 be met assuming a local area reduction of the pressure retaining membrane. Therefore, the maximum allowable end-of-evaluation period flaw size is also determined using the primary stress limit and is compared to the maximum allowable end-of-evaluation period flaw sizes determined for all normal/upset/test and emergency/faulted condition transients. The primary stress limit calculation was found to be more governing than the ASME Section XI Paragraphs IWB-3611 or IWB-3612 acceptance criteria, and limited the flaw depth to 22.5% of the pressurizer lower head thickness. This limiting maximum allowable end-of-evaluation period flaw size is used in the creation of the crack growth chart.

4.4.2 Crack Growth Chart

Once the maximum allowable end-of-evaluation period flaw sizes are determined, crack growth analyses are performed according to the methodology discussed in Section 4.3. The crack growth analyses are performed to determine the flaw size as a function of time, which can be compared to the maximum allowable end-of-evaluation period flaw sizes to determine the acceptability of abandoning a flaw in the heater sleeve attachment weld as-is. The initial flaw will be postulated to the depth equal to the partial penetration weld plus cladding thickness, thus, the flaw tip is at the inside surface of the pressurizer lower head base material. Crack growth is determined for both the uphill and downhill sides of the heater sleeve and the most limiting results are used in the creation of the crack growth chart.

The fatigue crack growth rate based on ferritic steel in water is used along with the corrosion crack growth rate. The fatigue crack growth evaluation requires pressure loading and hoop transient stresses.

The crack growth for the pressurizer lower head at the location of the heater sleeve penetrations is shown in Figure 4-4. The vertical axis of the flaw chart shows the flaw depth (a) to wall thickness (t) ratio; for example, a/t = 0.1 is a 10% through-wall flaw and a/t = 0.2 is a 20% through-wall flaw. The horizontal axis displays the operation duration.

Acceptability of abandoning the original heater sleeve attachment weld can be determined by using the crack growth chart to compare the final flaw size after the remaining operation duration of the plant to the maximum allowable end-of-evaluation period flaw size.

Based on the crack growth chart, it would take more than 40 years for the postulated flaw in the heater sleeve attachment weld to grow into the pressurizer lower head and reach a size that would be considered unacceptable according to Section XI of the ASME Code. Therefore, according to Figure 4-4, it can be demonstrated that a flaw in the heater sleeve attachment weld will not grow to a size that would violate the ASME Section XI flaw size criteria before the end of plant life and the flawed attachment weld may be abandoned for the remaining life of the plant.

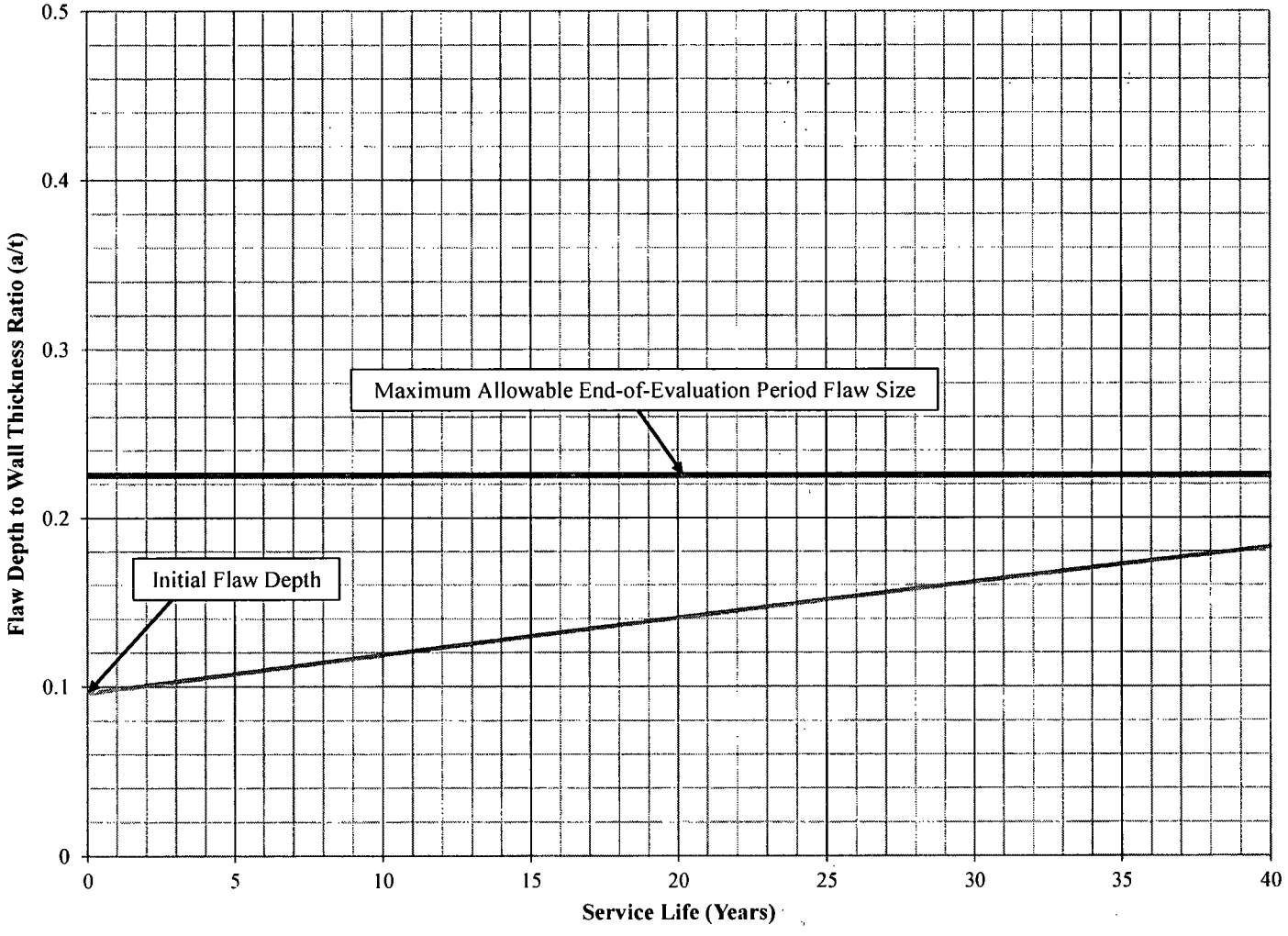

Figure 4-4 Crack Growth for Turkey Point Units 3 and 4 Pressurizer Lower Head

5 SUMMARY AND CONCLUSION

During the Spring 2014 refueling outage at Turkey Point Unit 3, a pressure boundary leak was discovered in the #11 pressurizer heater sleeve. No flaws were identified in the heater sleeve material through non-destructive examination, and it was assumed that the partial penetration weld between the cladding and heater sleeve on the inside of the pressurizer bottom head is flawed. The existing nozzle was removed to approximately half the thickness of the pressurizer head and a new nozzle inserted. The pressure boundary weld was relocated to the outside surface of the pressurizer lower head and the assumed flawed partial penetration weld and a portion of the existing nozzle was abandoned in place.

A flaw stability analysis is performed in this report to evaluate the long-term operating life of the pressurizer lower head based on ASME Section XI IWB-3600 [1] guidelines and determine the acceptability of abandoning a flawed partial-penetration weld for the life of the Turkey Point Units 3 and 4. To support the fracture mechanics evaluation, a three-dimensional FEM of the pressurizer lower head and heater sleeve penetration was created to determine the through-wall time history stresses in the region of the lower head near the location of the heater sleeves. The stress results from the finite element modeling, which are discussed in Section 3, are used as input to the fracture mechanics evaluation. The evaluation provided herein is based on the geometry and stresses for the outermost row of heater sleeve penetrations and the results envelop all heater penetration rows. Therefore, the evaluation contained herein is applicable to all heater sleeve penetrations in the Turkey Point Units 3 and 4 pressurizer lower heads.

The pressurizer lower head in the region of the heater sleeve penetrations has been evaluated in accordance with the ASME Section XI in-service inspection acceptance criteria and a crack growth chart has been developed for the Turkey Point Units 3 and 4 pressurizer lower head. The crack growth chart shown in Figure 4-4 determines crack growth based on an initial flaw depth that extends to the cladding to base metal interface. Crack growth is calculated into the pressurizer lower head based on the combination of fatigue and corrosion cracking. According to the crack growth chart in Figure 4-4, and the results in Table 5-1, it would take more than 40 years for a flaw which encompasses the entire original heater sleeve attachment weld to grow beyond the ASME Section XI Code maximum allowable flaw size. Turkey Point Units 3 and 4 have less than 40 years of operation remaining, including license renewal. Therefore, a flawed heater sleeve partial penetration weld is shown to be acceptable per Section XI of the ASME Code for the remaining life of the plant.

Table 5-1 Turkey Point Units 3 and 4 Pressurizer Heater Sleeve Attachment Weld Crack Growth Results

Flaw Size (a/t)			Maximum Allowable End-of-Evaluation Period Flaw Size (a/t)
Initial	20 Years	40 Years	
0.096	0.141	0.183	0.225

An additional investigation was performed to determine the corrosion rate required to cause the postulated flaws to reach the maximum allowable end-of-evaluation period flaw size within 40 years. When combined with fatigue crack growth, a corrosion rate of [ ]^{a,c,e} mils per year would cause the postulated flaw to reach the maximum allowable end-of-evaluation period flaw size (a/t = 0.225) in 40 years, which corresponds to the plant operation in the full power mode for [ ]^{a,c,e} of the time ([ ]^{a,c,e} mils per year corrosion rate) and in the startup mode for [ ]^{a,c,e} of the time ([ ]^{a,c,e} mils per year corrosion rate). These values are conservatively determined using only operating condition and startup condition corrosion rates from WCAP-15973-P. The corrosion rate at the startup condition is more conservative than the corrosion rate at the refueling condition. Any time spent in the refueling mode would reduce the amount of time required at full power operation.

Furthermore, it was determined that the heater sleeve bore diameter remains acceptable, even with corrosion, beyond the remaining lives of Turkey Point Units 3 and 4. For the heater sleeve hole diameter to reach the maximum allowable diameter within 20 years, Turkey Points Units 3 and 4 would have to operate at full power for [ ]^{a,c,e} of the time. For the heater sleeve hole diameter to reach the maximum allowable diameter within 40 years, Turkey Points Units 3 and 4 would have to operate at full power for [ ]^{a,c,e} of the time. These values are conservatively determined using only operating condition and startup condition corrosion rates from WCAP-15973-P, and any time spent in the refueling mode would reduce the amount of time required at the full power operation condition. Both of these operation time splits are conservative and bounded by the current Turkey Point Units 3 and 4 power capacity factors.

6 REFERENCES

1. ASME Boiler and Pressure Vessel Code, Section XI, 2007 Edition with 2008 Addenda.

2. Florida Power and Light Letter, L-2014-096, "Turkey Point Unit 3, Docket No. 50-250, Inservice Inspection Plan – Fifth Inspection Interval Unit 3 Relief Request No. 1," April 4, 2014. NRC Accession Number: ML14098A036.

3. Westinghouse Engineering Report, WCAP-17152-P, Rev. 1, "Turkey Point Units 3 and 4 Extended Power Uprate (EPU) Engineering Report," December 4, 2014. (Westinghouse Proprietary Class 2)

4. Westinghouse Letter, LTR-CPS-08-118, Rev. 2, "NSSS Design Transients for the Turkey Point Units 3 and 4 EPU Program," October 30, 2014. (Westinghouse Proprietary Class 2)

5. Westinghouse Report, WCAP-15370, Volume 1, Rev. 0, "Turkey Point Units 3 and 4 Design Basis Transient Evaluation for License Renewal," January 31, 2000. (Westinghouse Proprietary Class 2)

6. Westinghouse Systems Standard, SSDC 1.3, Rev. 1, "Systems Standard Design Criteria Nuclear Steam Supply System Design Transients," April 5, 1971. (Westinghouse Proprietary Class 2)

7. Florida Power and Light Letter, PTN-ENG-15-0001, "Response to Email Requests to Define the Turkey Point Unit 3 and 4 Operating Transients Applicable to the Pressurizer Heater Sleeve Flaw Evaluation," January 7, 2015.

8. Westinghouse Report, WCAP-14950, Rev. 0, "Mitigation and Evaluation of Pressurizer Insurge/Outsurge Transients," February 25, 1998. (Westinghouse Proprietary Class 2)

9. Westinghouse Drawings:

   a) 681J271, Rev. 6, "General Assembly & Final Machining."

   b) 681J252, Rev. 5, "Lower Head Ass'y. & Details."

   c) 4417D30, Rev. 8, "Outline."

   d) 632C552, Rev. 13, "Heater Well Assy."

   e) 4417D12, Rev. 8, "Lower Head Casting."

   f) 675J675, Rev. 3, "General Assy. & Final Mach."

   g) 679J454, Rev. 8, "Lower Head Ass' & Dets."

10. Westinghouse Report, WNET-114-P-3-13, Rev. 0, "Series 84 Pressurizer Stress Report: Immersion Heater Analysis," June 1973. (Westinghouse Proprietary Class 2)

11. Structural Integrity Associates Calculation Number, FPL-09Q-307, Rev. 0, "Pressurizer Insurge/Outsurge Fatigue Analysis," August 1, 2000.

12. American Petroleum Institute, API 579-1/ASME FFS-1 (API 579 Second Edition), "Fitness-For-Service," June 2007.

13. *Flaw Evaluation Procedures: ASME Section XI.* Electric Power Research Institute , Palo Alto, CA: August 1978. NP-719-SR.

14. Westinghouse Report, WCAP-15973-P-A, Rev. 0, "Low-Alloy Steel Component Corrosion Analysis Supporting Small-Diameter Alloy 600/690 Nozzle Repair/Replacement Programs," February 2005. (Westinghouse Proprietary Class 2)

15. Westinghouse Letter, LTR-MRCDA-14-32, Rev. 0, "Westinghouse Support of FPL Response to NRC RAI Question 3 for Turkey Point Unit 3 Fifth Inspection Interval Relief Request No. 1 (MF3834)," April 9, 2014.

16. Westinghouse Calculation Note, CN-MRCDA-14-27, Rev. 0, "Turkey Point Units 3 and 4 Pressurizer Heater Sleeve Stress Analysis," January 29, 2015. (Westinghouse Proprietary Class 2)

17. Westinghouse Calculation Note, CN-PAFM-15-1, Rev. 0, "Turkey Point Units 3 and 4 Pressurizer Heater Sleeve Penetration Half-Nozzle Repair Flaw Evaluation," February 11, 2015. (Westinghouse Proprietary Class 2)

18. Westinghouse Engineering Report, WCAP-17846-P, Rev. 0, "Technical Basis for Westinghouse Embedded Flaw Repair for Hanbit Unit 4 Reactor Vessel Head Penetration Nozzles," December 2013. (Westinghouse Proprietary Class 2)